Atmospheric Dynamics of Terrestrial Planets

Peter L. Read, Stephen R. Lewis, and Geoffrey K. Vallis

Contents

Abstract

The solar system presents us with a number of planetary bodies with shallow atmospheres that are sufficiently Earth-like in their form and structure to be termed "terrestrial." These atmospheres have much in common, in having circulations that are driven primarily by heating from the Sun and radiative cooling to space, which vary markedly with latitude. The principal response to this forcing is typically in the form of a (roughly zonally symmetric) meridional overturning

P. L. Read (✉)
Atmospheric, Oceanic & Planetary Physics, Clarendon Laboratory, University of Oxford, Oxford, UK
e-mail: peter.read@physics.ox.ac.uk

S. R. Lewis
School of Physical Sciences, Faculty of Science, Technology, Engineering and Mathematics, The Open University, Milton Keynes, UK
e-mail: stephen.lewis@open.ac.uk

G. K. Vallis
College of Engineering, Mathematics and Physical Sciences, University of Exeter, Exeter, UK
e-mail: G.Vallis@exeter.ac.uk

© Springer International Publishing AG, part of Springer Nature 2018
H. J. Deeg, J. A. Belmonte (eds.), *Handbook of Exoplanets*,
https://doi.org/10.1007/978-3-319-30648-3_50-2

that transports heat vertically upward and in latitude. But even within the solar system, these planets exhibit many differences in the types of large-scale waves and instabilities that also contribute substantially to determining their respective climates. Here we argue that the study of simplified models (either numerical simulations or laboratory experiments) provides considerable insights into the likely roles of planetary size, rotation, thermal stratification, and other factors in determining the styles of global circulation and dominant waves and instability processes. We discuss the importance of a number of key dimensionless parameters, for example, the thermal Rossby and the Burger numbers as well as nondimensional measures of the frictional or radiative timescales, in defining the type of circulation regime to be expected in a prototypical planetary atmosphere subject to axisymmetric driving. These considerations help to place each of the solar system terrestrial planets into an appropriate dynamical context and also lay the foundations for predicting and understanding the climate and circulation regimes of (as yet undiscovered) Earth-like extrasolar planets. However, as recent discoveries of "super-Earth" planets around some nearby stars are beginning to reveal, this parameter space is likely to be incomplete, and other factors, such as the possibility of tidally locked rotation and tidal forcing, may also need to be taken into account for some classes of extrasolar planet.

Introduction

Mars, Venus, Earth, and Titan present us with four clear examples in the Solar System of rocky planetary bodies with shallow, though substantial, atmospheres. Such bodies are often termed "terrestrial planets" because of their similarities to Earth and to contrast them with other classes of planets, such as the gas giants and ice giants. This class of planetary atmosphere may be supplemented in the Solar System by two other examples on Pluto and Triton, the largest moon of Neptune, which have more tenuous and ephemeral atmospheres but which nevertheless may exhibit dynamic circulation systems that affect their surfaces. Titan and Triton are not strictly "planets" using the definition of the International Astronomical Union because they do not directly orbit the Sun, and Pluto is officially a *dwarf planet* because it is not big enough to clear its orbit. Nevertheless, we may informally refer to all of them as *terrestrial planets* so far as their atmospheres are concerned. The form and strength of their atmospheric circulations differ significantly, however, and a clear goal of studies in planetary atmosphere dynamics should be to ascertain what are the dominant factors governing both the similarities and differences in their styles of global circulation.

To some extent, this question can be addressed from a knowledge of basic fluid dynamics, radiative transfer, and thermodynamics, taking into account the differing sizes, compositions, and rotation state of each planet. Thus, atmospheric motions on more rapidly rotating planets such as Earth or Mars are likely to be in geostrophic balance, with horizontal pressure gradient forces (per unit mass) in approximate balance with Coriolis accelerations, while on slowly rotating bodies, such as Venus or Titan, Coriolis accelerations are too weak to balance pressure gradients, and their place is taken by centrifugal accelerations, at least in the zonal (east-west) direction (Leovy 1973). But more subtle differences, such as how heat and momentum are distributed around the planet, how widely do meridional overturning circulations extend across the planet, and what kind of waves and instabilities may play important roles in the circulation, are more difficult to answer without resort to more complex numerical and mathematical models.

While at first sight it might seem that the modern approach to such questions should be to construct and run vastly complex and detailed computer simulations of the atmospheric system in question, such an approach is likely to offer little in the way of understanding and insight into what may be the most important processes and factors governing the basic circulation regime obtained. For such insights it is much preferable to make use of simplified model systems that allow us to represent a hypothetical subset of key processes within a framework that enables us to run sequences of controlled "experiments" (either numerically or in a laboratory) and to make a connection to fundamental theory . Through this means, we may evaluate the parametric dependence of various factors in the circulation, and conduct sensitivity studies to investigate the impact of adding further layers of complexity, thus gaining insight as to what factors are either essential or peripheral to the circulation phenomena in question.

Such an approach has a long history in certain areas of science and, in particular, in geophysical fluid dynamics (Vallis 2016). Controlled experiments on convection in rotating, stably stratified fluids have been carried out in the laboratory for many years (e.g., Hide 1953; Fultz et al. 1959), in which the occurrence of a range of different flow regimes and phenomena was mapped systematically within a suitably defined parameter space. Although the systems studied in the laboratory, typically in the form of viscous liquids confined within cylindrical tanks on rotating tables, appear at first sight to bear little resemblance to a planetary atmosphere, they are remarkably successful in capturing much of the essential physics underlying global atmospheric circulation patterns driven by differential solar heating. Such studies provided invaluable sources of insight during the development of dynamical meteorology for Earth in the 1950s and 1960s, as discussed, e.g., by Lorenz (1969), Lorenz (1993) and Hide and Mason (1975), and research on these kinds of system continues fruitfully to the present day (e.g., Read 2001; Wordsworth et al. 2008; Read et al. 2015, and references therein).

This parametric approach has also been applied to atmospheric circulation regimes using simplified numerical simulation models, and this has led to a steady trickle of studies during the past 30–40 years (Williams and Holloway 1982; Geisler et al. 1983; Del Genio and Suozzo 1987; Williams 1988a,b; Jenkins 1996; Navarra and Boccaletti 2002; Mitchell and Vallis 2010; Kaspi and Showman 2015; Wang et al. 2018), stimulated by a variety of considerations ranging from fundamental studies in circulation theory or numerical model testing to planetary atmospheres and terrestrial paleoclimate. As we discuss below, the results of these model studies do serve to demonstrate a range of important trends in the way global atmospheric circulation systems evolve in response to changes in some of the basic planetary parameters.

These kinds of circulation regime studies have recently been given a new topicality with the developing discoveries of planets around other nearby stars (e.g., see http://exoplanet.eu/), including more than 200 rocky planets of comparable size to Earth (e.g., Beaulieu et al. 2006; Udry et al. 2007; Mayor et al. 2009) up to the time of writing. The confirmed existence of such planets greatly expands the likely range of parameters that need to be explored if the climate and circulation, and hence the potential habitability, of such planets are to be understood and quantified. But much depends on the style of atmospheric circulation on these planets and the efficiency of heat transport, e.g., between equator and poles, as to whether a climate potentially benign to life might exist on these bodies.

In this article we briefly review and discuss the range of dynamical circulation regimes that are observed in terrestrial planets and/or are found in simplified general circulation model simulations. Section "Global Circulation Patterns on Solar System Terrestrial Planetary Bodies" briefly introduces the main features of the global circulations of Earth, Mars, Pluto, Triton, Titan, and Venus, outlining the kinds of similarities and differences that need to be understood. In section "Circulation Regimes in Atmospheric Models" we go on to define corresponding dimensionless variables for fully spherical planetary atmospheres and review some of the trends emerging from such model regime studies. These are used to illustrate how these dimensionless parameters can provide order to the corresponding parameter space for atmospheric models, with regimes that also resemble those found in the laboratory. Finally, we provide some concluding remarks and discussion in section "Discussion".

Global Circulation Patterns on Solar System Terrestrial Planetary Bodies

The basic circulations of the atmospheres of all the terrestrial planetary bodies within the Solar System share a number of features in common. With the exception of Pluto (obliquity $\sim 60°$ or $120°$ taking into account its retrograde rotation), their obliquities (relative to their orbits about the Sun) lie within the fairly narrow range of $3°$–$30°$, ignoring the retrograde rotations of Venus, Pluto, and Triton (see Table 1). Thus, when averaged over their orbital period around the Sun, their tropical regions are heated more strongly by solar radiation than the poles. The principal driving force for their atmospheric circulations is therefore a result of differential solar heating between the equator and poles. This will lead to a general tendency for atmospheric motions to organize themselves in order to transport heat from the tropics toward the poles. Such transport is then inhibited to a greater or lesser extent depending (among other things) on the rate of planetary rotation.

In the absence of other constraints, the basic pattern of differential heating and cooling with latitude will tend to produce an overturning circulation that is more

Table 1 Planetary and orbital parameters for terrestrial-style solar system bodies with substantial atmospheres, ordered by rotation rate. The values given for the obliquities of Titan and Triton are those of Saturn and Neptune, respectively, with the obliquity of Titan and Triton with respect to their orbits around those planets given in brackets

Body	Mean radius (km)	Rotation period (h)	Solar day (h)	Obliquity (°)
Earth	6371	23.9	24.0	23.45
Mars	3396	24.6	24.7	25.2
Pluto	1151	154	154	119.6
Triton	1353	141	141	29.56(< 1)
Titan	2575	383	383	26.73(< 1)
Venus	6051	5833	2802	177.4

or less axisymmetric about the polar axis (provided diurnal effects are weak), with rising motion close to the equator and sinking motions at higher latitudes. Such a circulation pattern is known as a Hadley circulation, after the English explorer, James Hadley, who explained the tropical trade winds in the eighteenth century based on arguments invoking this type of circulation pattern. The influence of the Coriolis effect on meridional motions will lead naturally to the generation of east-west (zonal) flow. The tendency of parcels of air to conserve their angular momentum per unit mass also leads naturally to an increase in zonal flow relative to the underlying planet with latitude away from the equator, tending to form subtropical zonal (east-west) jet streams.

Table 2 lists some of the main flow phenomena seen in the four best-observed terrestrial atmospheres. The lists are not intended to be exhaustive but include the main axisymmetric zonal and meridional flows as well as commonly occurring wave or eddy phenomena. As will be discussed in more detail in subsequent sections, the flows seen in solar system atmospheres tend to fall into several categories according to the rotation rate of the underlying solid body. Earth and Mars are the two most rapid rotators, both with periods of about 24 h (Table 1) although the radius of Mars is only a little over half that of Earth so that its effective rotation, as represented by the thermal Rossby number (discussed in section "Circulation Regimes in Atmospheric Models") is much less than that of Earth. Nevertheless, Earth and Mars have much in common, with the jet streams that form as air moves away from the equator readily becoming unstable to potential energy-releasing baroclinic disturbances, leading to more complicated, non-axisymmetric flows and meanders in the subtropical and high-latitude jets. The detailed behavior of their atmospheres differs as a result both of the smaller radius of Mars and the lower thermal inertia of the Martian atmosphere and surface. Earth also has oceans with a large heat capacity that tempers the seasons, whereas on Mars the circulation differs considerably between seasons, with mainly weak easterly flow in the summer hemisphere and very little, if any, baroclinic wave activity, in stark contrast to the winter hemisphere which is dominated by strong westerly flow at midlatitudes and active baroclinic storms.

The second pair of atmospheres listed in Table 2 are those of the slow rotators, Titan and Venus. These both exhibit very strong atmospheric super-rotation, in other

Table 2 Some observed atmospheric phenomena on Earth, Mars, Titan, and Venus, partially categorized by approximate latitude bands (the precise regions vary and may be seasonal)

Body	Low-latitude (∼0–30°)	Midlatitude (∼30–60°)	High-latitude (∼60–90°)
Earth	Hadley circulation	Subtropical jet and westerlies	Polar jet stream and vortex
	Walker circulation	Extratropical cyclones and	Polar lows
	Tropical cyclones	anticyclones Baroclinic	Polar front
	Monsoons	turbulence and frontal systems	
	Moderate seasonal cycle – obliquity 23° – but tempered by oceans		
	Water is a condensate existing in solid, liquid, and vapor forms		
	Active hydrology cycle at all latitudes		
	Of the solar system planets, only Titan and Earth have liquid at the surface		
Mars	Cross-equatorial Hadley cell	Extended Hadley cell	Polar vortex in winter
	Thermal tides	Westerly jet in winter	Polar lows
	Dust storms	Baroclinic waves and eddies	Polar cap edge dust storms
		Dust storms	Polar hood clouds
	Strong seasonal cycle – obliquity 25°, eccentricity 0.09, no moderating oceans		
	Carbon dioxide is a condensate, existing mainly in gaseous and solid forms		
	Significant condensation and sublimation due to seasonal variations		
	Early Mars (3.5 bya) may have had liquid water on its surface		
Titan	Cross-equatorial Hadley cell	Extended Hadley cell	Polar vortex in winter
	Super-rotating zonal flow		
	Gravity waves		
	Strong seasonal cycle due to Saturn's obliquity (27°) and low surface heat capacity		
	Methane is a condensate, existing in both gaseous and liquid forms		
	Active seasonally varying methane cycle with the atmosphere transporting methane poleward, returning at the surface or subsurface and/or seasonally in the atmosphere		
Venus	Symmetric Hadley cells	Symmetric Hadley cells	Polar vortex
	Super-rotating zonal flow		
	Large-scale planetary waves,		
	topographic gravity waves		
	Very weak seasonal cycle – very low obliquity and eccentricity		
	Mainly dry atmosphere with a weak hydrology cycle		
	High (∼60 km) clouds of sulfuric acid droplets, but no condensate reaches the ground		

words prograde zonal flows with more angular momentum about the rotation axis than stationary air at the equator. The maximum local angular velocity (and specific angular momentum) of both atmospheres exceeds that of an atmosphere in solid body rotation with the underlying planet by more than 10 (Titan) or 60 (Venus) times. In contrast, Earth and Mars only exhibit weak, equatorial super-rotating jets (Lewis and Read 2003; Read and Lebonnois 2018). These jets are not unstable to baroclinic disturbances in the same way as on the rapid rotators, but planetary-scale waves (often symmetric about the equator in a "Y" shape) have been observed on

Venus (Sánchez-Lavega et al. 2017), and gravity-wave phenomena have been seen in the cloud decks of both bodies. Polar vortices are a common theme for all the bodies in Table 2, either stronger in winter, as on Earth, or likely only present in winter on Mars and Titan. Venus, with a much weaker seasonal cycle, has vortices at both poles, and they have been seen to form into patterns of two or three (a dipole or tripole) in an active process.

Pluto and Triton form a possible intermediate group but are not included in Table 2 since they have only been observed briefly for short portions of their seasonal cycle, but some numerical simulations of both will be shown below. Both bodies have relatively tenuous atmospheres that condense and sublimate over the seasonal cycle, leading to circulations that primarily transport mass from pole to pole.

Many of the features mentioned in Table 2 and discussed above can be seen in the observed annual-mean circulation of Earth's atmosphere (see Fig. 1; Kållberg et al. 2004, Schneider 2006). The temperature field (Fig. 1a) shows a clear tendency for temperature to decrease away from the equator toward both poles in the troposphere ($p > 100$ hPa) though with a more complicated (partly reversed) thermal gradient at higher altitudes. The meridional circulation (as seen in the mass streamfunction, defined such that $\rho \mathbf{u} = \mathbf{j} \times \nabla \psi$, where ρ is the density of the air and ψ is the streamfunction; see Fig. 1b) shows that a thermally direct Hadley circulation forms in each hemisphere, roughly antisymmetric about the equator though with some irregularities and a small northward displacement related to the asymmetric distribution of continents at Earth's surface and extending to around 30–40° latitude in each hemisphere. At higher latitudes, however, there are additional (thermally indirect) circulation cells (Fig. 1b) that owe their existence to complex interactions between the zonal flow and baroclinically unstable eddies (e.g., see Andrews et al. 1987; Schneider 2006). The corresponding pattern of zonal flow (Fig. 1b) is concentrated into subtropical, eastward jets in the troposphere at around 30° latitude, with additional mesospheric jets at high altitudes and predominantly westward flow over the equator at all heights.

The annual- and zonal-mean atmospheric circulations of Mars show many similar features to Earth (see Fig. 2), with zonal mean temperature decreasing toward the poles in the lower atmosphere ($p > 10$ Pa) roughly symmetrically about the equator, strong eastward zonal jets at midlatitudes in both hemispheres and a similar pattern of meridional overturning circulation (Hadley) cells in the subtropics. There is even some evidence of thermally indirect meridional (Ferrel) cells at midlatitudes, as found on Earth, associated with the effects of baroclinic eddies. However, this annual-mean picture provides a somewhat misleading impression of similarity with Earth, because seasonal variations in this global circulation pattern are substantial and change the instantaneous form of the circulation very considerably from the patterns in Fig. 2 (Read and Lewis 2004), especially around the solstice seasons. At those times the meridional circulations take the form of a single, equator-crossing Hadley circulation associated with strong mass transport from one hemisphere to the other. The solstice is also characterized by large temperature differences between summer and winter hemispheres, with the summer pole being warmer than the

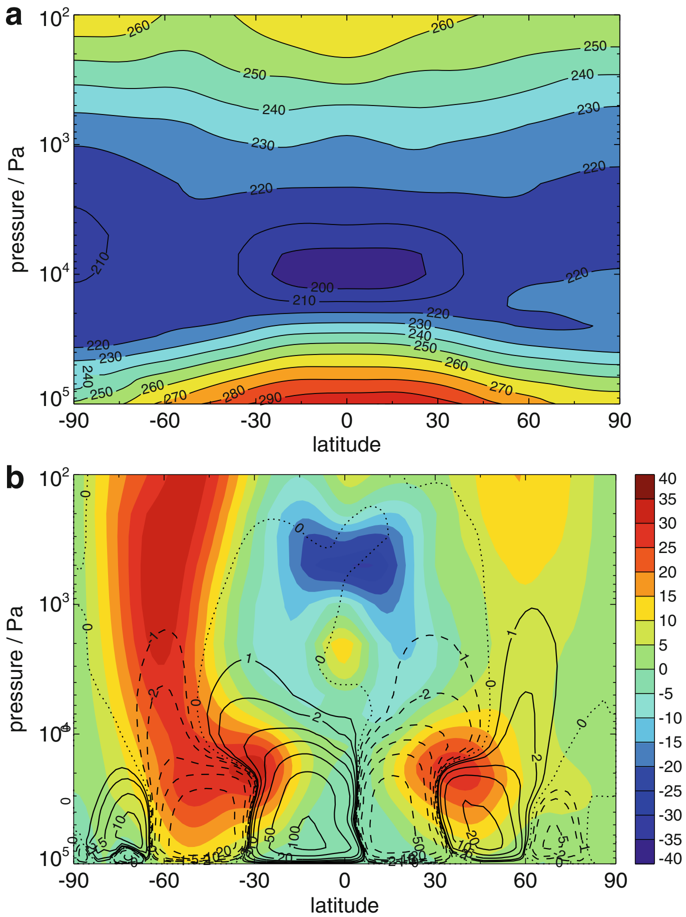

Fig. 1 Zonal and annual mean patterns of (**a**) temperature and (**b**) zonal wind (colors) and meridional mass streamfunction (contours, solid are positive or anticlockwise rotation, in units of 10^9 kg/s) for Earth's atmosphere in 2016 from the ERA40 reanalysis dataset (Dee et al. 2011) shown in meridional (latitude-height) cross section

tropics for a short time, strong eastward zonal winds in the winter hemisphere, and westward winds in the summer hemisphere. Such large changes are a consequence of the lack of oceans at the surface of Mars, which act to moderate seasonal temperature changes on Earth. In most respects, however, the basic circulation of both Earth and Mars are in reasonably similar regimes, characteristic of relatively rapidly rotating planets, with a tendency for large-scale wind patterns to be in geostrophic balance.

Venus and Titan, on the other hand, exhibit a rather different form of circulation pattern. As suggested from global circulation models (e.g., see Figs. 3 and 4;

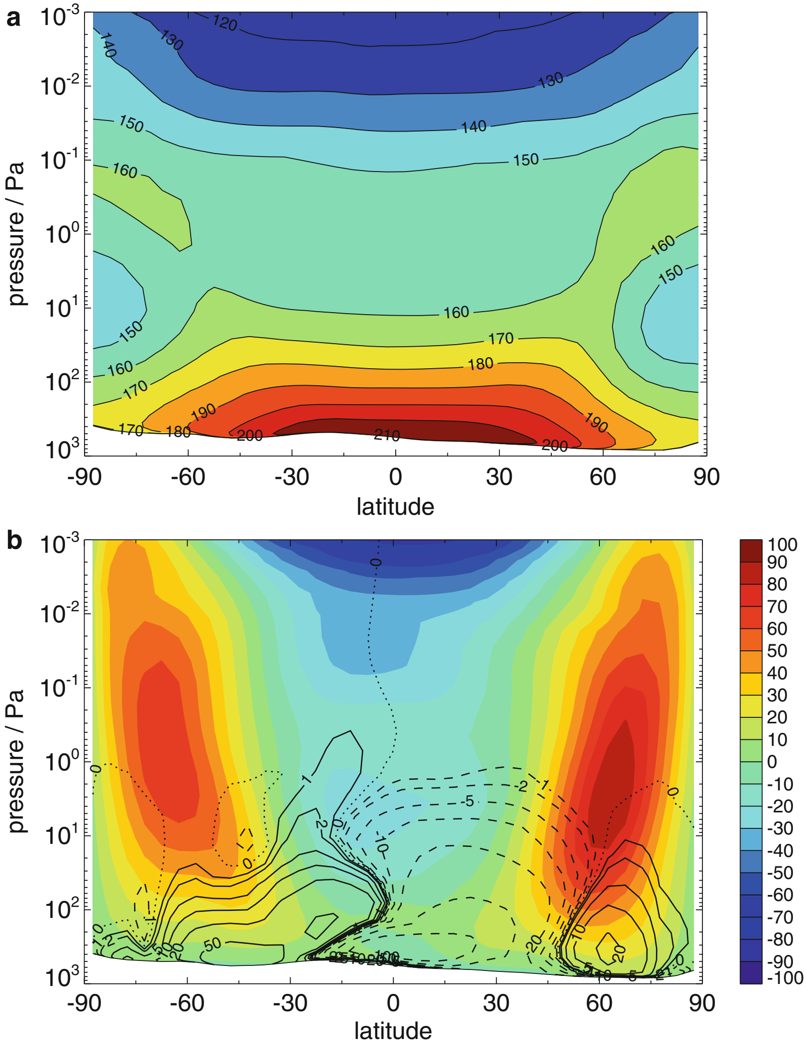

Fig. 2 Zonal and annual mean patterns of (**a**) temperature and (**b**) zonal wind (in color) and meridional mass streamfunction (contours, solid are positive or anticlockwise rotation, in units of 10^7 kg/s) for a typical year in the Martian atmosphere without a global dust storm, shown in meridional (latitude-pressure) cross section. Temperature and wind data used to form these plots are from the Mars Climate Database (Lewis et al. 1999; Read and Lewis 2004)

Lebonnois et al. 2010, 2012, 2016), the zonal mean flow on Venus is typically dominated by two large, thermally direct meridional Hadley cells that span almost the entire distance from the equator to each pole. This enables very efficient transport of heat from the equator to poles, leading to relatively weak thermal contrasts between tropics and polar regions (Fig. 3a) at almost all heights. The

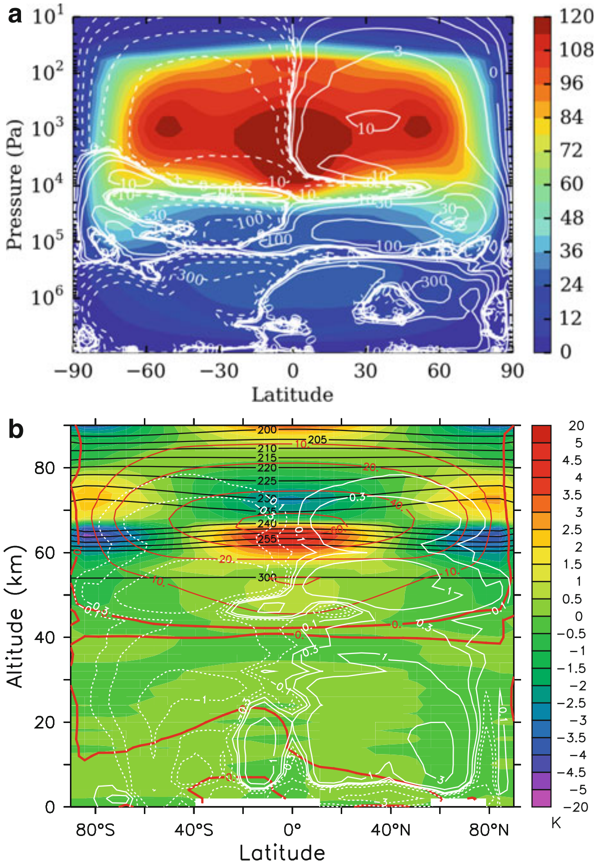

Fig. 3 Zonal mean patterns of (**a**) zonal wind (color shaded) and meridional mass streamfunction (white contours) and (**b**) temperature and latitudinal perturbations for the Venus atmosphere, shown in meridional (latitude-height) cross section. (**a**) is taken from Lebonnois et al. (2016) and (**b**) is from Lebonnois et al. (2010), respectively, with permission from Elsevier and the American Geophysical Union

most striking feature, however, is the presence of strong, prograde upper-level zonal winds at almost all latitudes, including on the equator itself. This apparent excess of atmospheric angular momentum at the equator, compared with the angular momentum air would have in the tropics in solid-body rotation with the underlying surface, is known as "super-rotation" (Read 1986; Read and Lebonnois 2018). The degree of super-rotation on both Venus and Titan is substantial, with zonal flows corresponding to angular rotation rates that are much faster than the underlying planet by at least an order of magnitude. This strong super-rotation implies that zonal winds cannot be in geostrophic balance but are more likely to be in a gradient wind or cyclostrophic balance between meridional pressure gradients and centrifugal accelerations. Seasonal variations appear to be weak on Venus, because

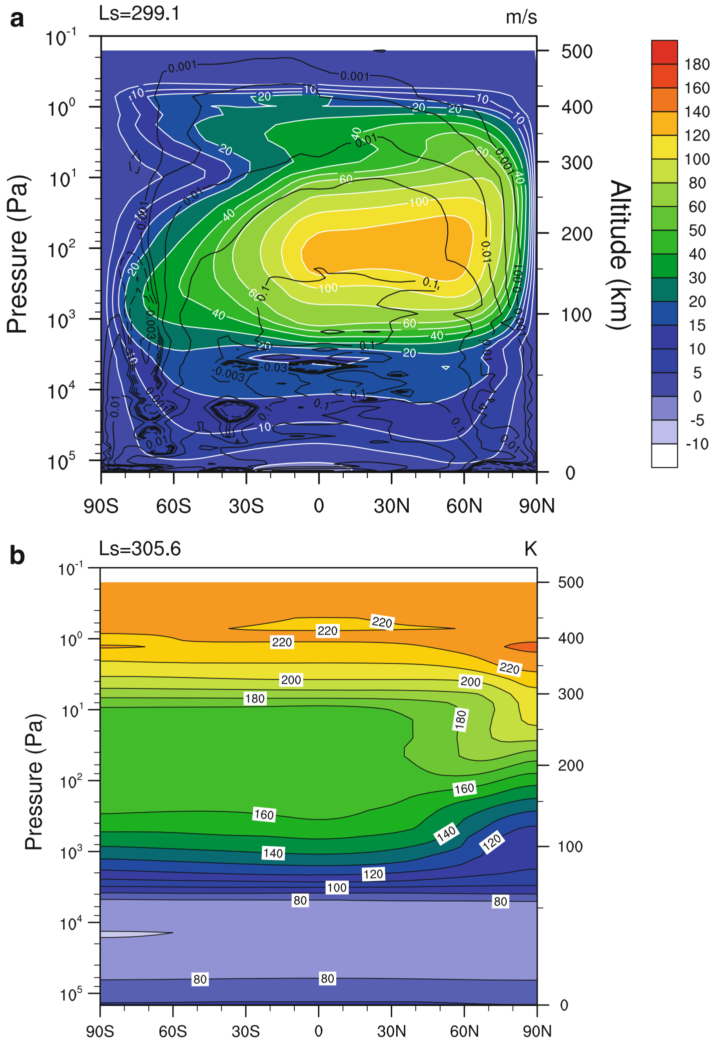

Fig. 4 Zonal mean patterns of (**a**) zonal wind (color shaded) and meridional mass streamfunction (black contours) and (**b**) temperature for Titan's atmosphere at $L_s \simeq 300°$, shown in meridional (latitude-height) cross section. (Figures are taken from Lebonnois et al. 2012, with permission from Elsevier)

of its very low obliquity, but rather more substantial on Titan (obliquity ~27°). Such seasonal variations lead to strong changes in the global circulation during the year, such that except close to equinox conditions, the meridional circulation is dominated by a single overturning cell with rising motion over the summer hemisphere and sinking motion during winter (see Fig. 4). Even during solstice, however, horizontal temperature gradients remain very small. This pattern of circulation, with large

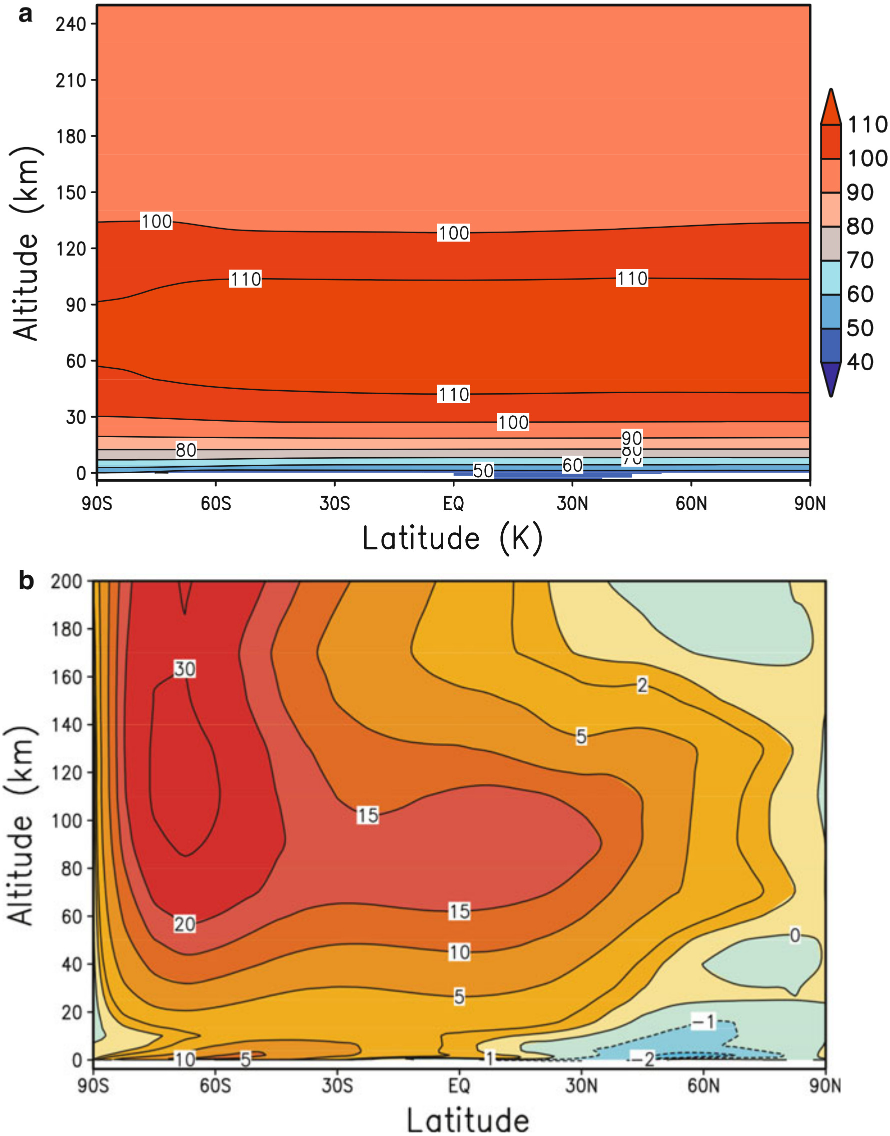

Fig. 5 Zonal mean patterns of (**a**) temperature and (**b**) zonal wind for Pluto's atmosphere around the time of the New Horizons encounter in 2015 (shortly after northern spring equinox so the south pole is cooling), shown in meridional (latitude-height) cross section. (Figures are taken from numerical climate model simulations by Forget et al. 2017, with permission from Elsevier)

hemispheric Hadley circulations, weak horizontal thermal gradients, and strong super-rotating winds, appears to be typical of slowly rotating planets, as we will see below (Fig. 5).

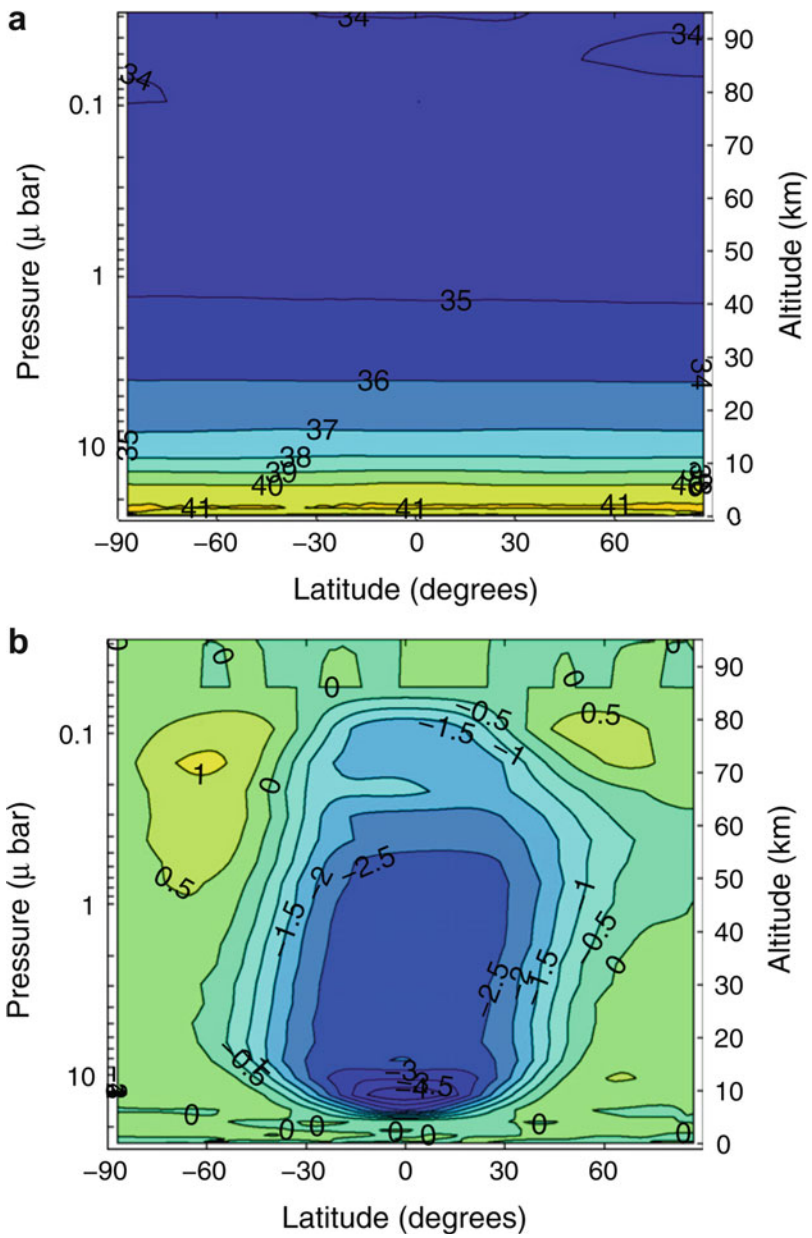

Fig. 6 Zonal mean patterns of (**a**) temperature and (**b**) zonal wind for Triton's atmosphere around the time of the New Horizons encounter in 2015 (approaching northern winter solstice), shown in meridional (latitude-height) cross section. (Figures are taken from numerical climate model simulations by Zalucha and Michaels 2013, with permission from Elsevier)

Given their relatively small sizes (radii of 1187 and 1353 km, respectively) and somewhat long (retrograde) rotation periods (6.40 and 5.88 Earth days, respectively), the atmospheres of Pluto and Triton appear to be intermediate in their circulations between Earth-like and Titan-like atmospheres. Both have substantial obliquities with respect to the Sun of around 30° (Triton) and 60° (Pluto – though it rotates in a retrograde sense relative to its orbit), so probably exhibiting significant seasonal variations. Both atmospheres consist largely of N_2 and other volatile organics and are sufficiently cold that significant portions of their atmospheres may condense onto the winter pole and then evaporate during their summers. Recent attempts to model their atmospheric circulations (e.g., Zalucha and Michaels 2013; Zalucha 2016; Forget et al. 2017) suggest that, despite these seasonal variations, horizontal thermal gradients are relatively weak, much like on Venus or Titan, with weak patterns of zonal winds that tend to peak near the equator except around solstices (Fig. 6). But in contrast to most other terrestrial solar system planets, their vertical temperature distributions evidently exhibit a strong inversion with altitude (e.g., Hubbard et al. 1990; Yelle et al. 1995). This results in a strong static stability that may inhibit vertical motions and a strong meridional overturning circulation. Models suggest, however, that the seasonal condensation flow has a much stronger influence on their circulation than is the case for Mars, and may even dominate the transport of angular momentum, though this is still rather uncertain.

Circulation Regimes in Atmospheric Models

The diversity of dynamical circulation regimes that is represented within the solar system, with several planetary circulations sharing some features in common but also with notable differences, raises the question as to whether at least some of these similarities and differences might be consistent with discernible trends, determined by key parameters defining the state of the system. Such trends are clearly observed in laboratory studies of rotating, stratified flows as parameters such as the rotation rate or size of the domain are varied, leading to well-characterized bifurcations or transitions between different flow states at critical values of these parameters (e.g., Hide and Mason 1975; Read et al. 2015).

One way in which this has been explored recently, in the same spirit of investigating bifurcations and transition between different flow regimes in laboratory systems, has been to examine the equilibrated circulation patterns obtained in numerical simulations using simplified global circulation models, in which certain key parameters (notably the planetary rotation rate) are varied. Studies of experimental analogues of atmospheric circulation systems have also been related to various idealized theoretical and model studies of nonlinear baroclinic wave interactions (e.g., see Ghil and Childress 1987), indicating that similar sequences of flow transitions from steady through regular, periodic to chaotic and turbulent flows should be generic to a wide variety of natural systems, presumably including atmospheric circulations (at least in principle). In this section, therefore, we look at some examples of model simulations using highly simplified GCMs that explore the

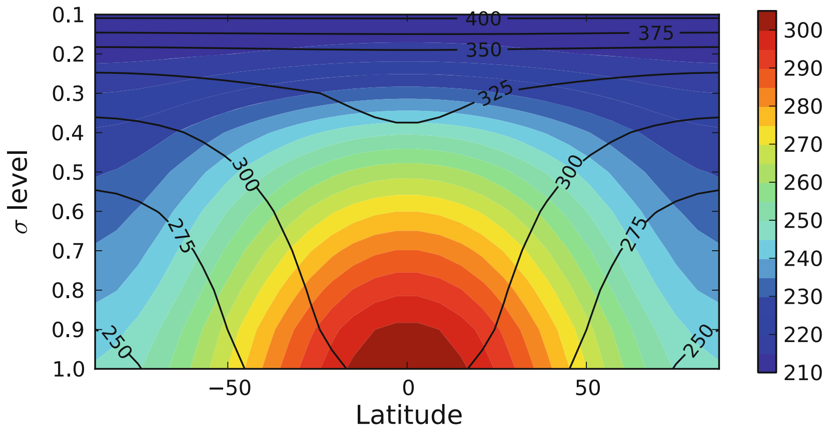

Fig. 7 Restoration temperature (color) and potential temperature (contour) field with equator-to-pole temperature difference of 60 K

extent to which some of the gross properties of the atmospheric circulations of solar system terrestrial planets can be related to the values of certain key parameters.

Circulation Regimes with Varying Rotation Rate

In the following, we illustrate these trends by showing a typical sequence of atmospheric model simulations for an Earth-sized planet with a shallow atmosphere, ordered by planetary rotation rate while keeping the thermal forcing fixed. The model used here is the pseudo-spectral Portable University Model of the Atmosphere (PUMA; e.g., see Fraedrich et al. 1998; Frisius et al. 1998; von Hardenberg et al. 2000). PUMA represents the dynamical core of a spectral atmospheric general circulation model (AGCM), following Bourke (1974) and Hoskins and Simmons (1975). Horizontal structures are represented as a series of projections onto a spectrum of spherical harmonics, while the vertical is divided into a number of equally spaced σ levels (where $\sigma = p/p_s$, where p and p_s denote the pressure and the surface pressure, respectively). A circulation is driven by a pattern of thermal forcing in which atmospheric temperature is relaxed linearly toward a prescribed distribution of temperature, whose form is shown in Fig. 7. This is intended to approximate to the annually averaged thermal state of Earth's atmosphere, with a relaxation timescale, τ_R, set to 30 Earth days in the free atmosphere, decreasing to 2.5 Earth days at $\sigma = 1.0$. The model also includes a simple Rayleigh friction boundary layer and hyperdiffusive dissipation (see Wang et al. 2018 for more details).

In order to explore a range of parameters, the model was run over a wide range of Ω, ranging from $\Omega_E/16$ to $8\Omega_E$ (where Ω_E is Earth's current rotation rate). Figure 8 presents the zonal mean zonal wind and temperature fields, respectively, from the

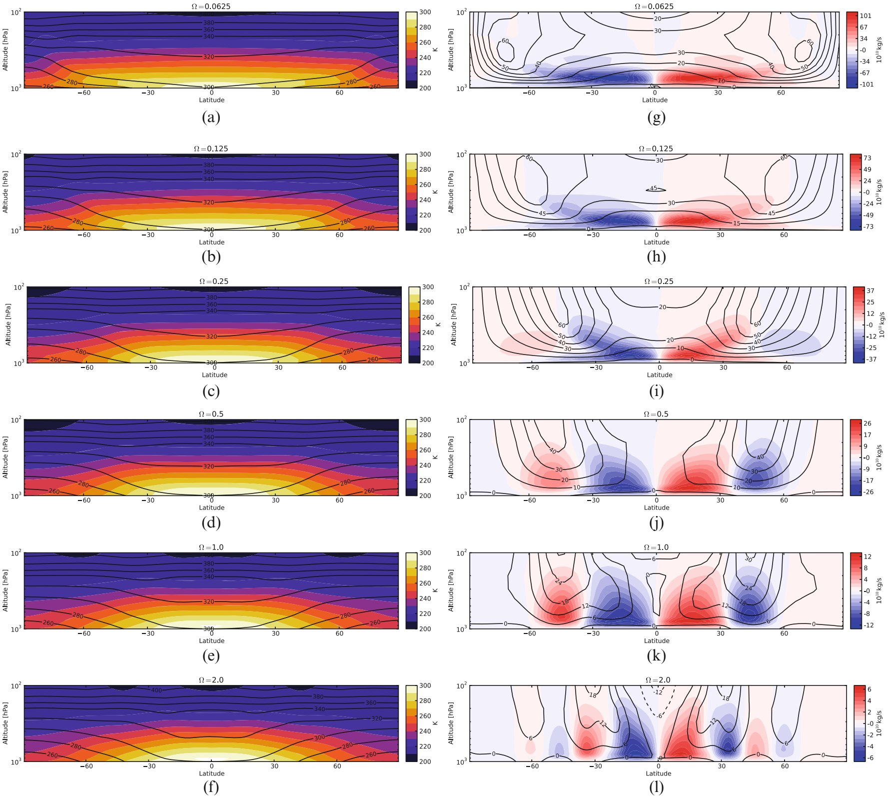

Fig. 8 Zonal mean fields of temperature (absolute, T, and potential, θ) [(**a**) – (**f**)] and zonal wind and meridional streamfunction [(**g**) – (**l**)] for $\Omega^* = 1/16$ [(**a**) & (**g**)], 1/8 [(**b**) & (**h**)], 1/4 [(**c**) & (**i**)], 1/2 [(**d**) & (**j**)], 1 [(**e**) & (**k**)], and 2 [(**f**) & (**l**)]. Shading indicates absolute temperature in (**a**) – (**f**) and meridional streamfunction in (**g**) – (**l**), while contours indicate potential temperature [(**a**) – (**f**)] and zonal velocity [(**g**) – (**l**)]

main sequence of simulations from Wang et al. (2018), which nicely illustrate a number of significant trends in circulation style and structure as Ω is varied. In particular, it is clear from Fig. 8 that, as $\Omega^* = \Omega/\Omega_E$ is reduced from $\Omega^* = 1$ or 2, the midlatitude prograde jet stream in each hemisphere migrates poleward from the subtropics, and overall flow becomes increasingly prograde at almost all latitudes and heights. This culminates in a strong (>80 m s^{-1}) circumpolar jet stream dominating the circulation at $\Omega^* = 1/16$. Broadly consistent results were also found by Potter et al. (2014).

Prograde flow is found on the equator at upper levels at almost all values of $\Omega^* < 1/2$. This gradually gives way with increasing Ω^* to equatorial sub-rotation, which is consistent with what is observed for Earth itself (cf. Fig. 1a), except during the westerly phase of the quasi-biennial oscillation (see, e.g., Andrews et al. 1987 or Vallis 2017). The presence of prograde flow on the equator is a clear indication of local super-rotation, defined as an excess of specific angular momentum (AM) compared to what the flow would have in solid body corotation with the underlying surface (Read 1986; Read and Lebonnois 2018) and represented by the dimensionless ratio, s, of that AM excess to the corotating value. This excess is typically very small for Earth, though some modeling studies have indicated the possibility of a bifurcation to an alternative circulation regime (Suarez and Duffy 1992; Saravanan 1993; Williams 2003; Kraucunas and Hartmann 2005) characterized by significant equatorial super-rotation at upper levels. Some models (Suarez and Duffy 1992; Saravanan 1993; Kraucunas and Hartmann 2005) suggest that this may be produced by non-axisymmetric heating in the tropics, although the model of Williams (2003) seems to generate super-rotation through low-latitude barotropic instability.

As Ω^* is increased beyond 1, however, there is a trend toward increasing numbers of parallel, zonal jet streams across the hemisphere which alternate in sign toward the pole, somewhat similar to the pattern of jets found on the rapidly rotating gas giant planets. The jets tend to increase in strength with altitude, peaking in the lower stratosphere, and are almost certainly driven by interactions with baroclinic eddies.

The corresponding temperature fields in Fig. 8 also show some interesting trends that follow a somewhat similar pattern to what is found in laboratory analogues. Thus, decreasing Ω^* below 1 initially leads to a reduction in the slope of the isotherms in the troposphere, though this increases again as Ω^* is changed from 1/2 to 1/4. The reduction in isotherm slope between $\Omega^* = 1/4$ and 1/2 is associated with the onset of geostrophic baroclinic instability around $\Omega^* \leq 1/2$ (Williams 1988a), roughly consistent with other studies (e.g., by Geisler et al. 1983, Del Genio and Suozzo 1987, and Navarra and Boccaletti 2002 who found an onset of baroclinic instability around $\Omega^* = 1/4$). Further reductions in Ω^* seem then to lead to a monotonic reduction of isotherm slope until, at $\Omega^* = 1/16$, the isotherms are almost entirely horizontal except close to the pole $\phi > 60°$. As Ω^* is increased beyond 1, however, the tropospheric isotherm slope tends to increase and develop step-like features at various latitudes that correlate with the appearance of alternating baroclinic zonal flows. This appears to be associated with the formation of parallel baroclinic zones which become separately unstable and evolve as a highly anisotropic form of geostrophic turbulence, with many similarities to the baroclinically unstable flows found in recent laboratory studies with sloping endwall boundaries (cf. Bastin and Read 1998; Wordsworth et al. 2008). Such similarities would strongly suggest a common role for strong and complex nonlinear wave-zonal flow interactions, modified by the β-effect, in producing the strongly zonal organization of the flow.

Figure 9 presents a series of instantaneous snapshots of the zonal velocity, u, at the top of the troposphere for each value of Ω^*, and provides an impression of the typical form of the dominant eddies in each regime. This shows the principal eddies at low rotation rates $\Omega^* \lesssim 1/4$ to manifest as an irregular meander of the main circumpolar jet stream with a zonal wavenumber $m = 1 - 2$. These meanders take a qualitatively different form around $\Omega^* = 1/2$, becoming much more symmetrical and regular in both space and time. By $\Omega^* = 1$, the meanders have increased in

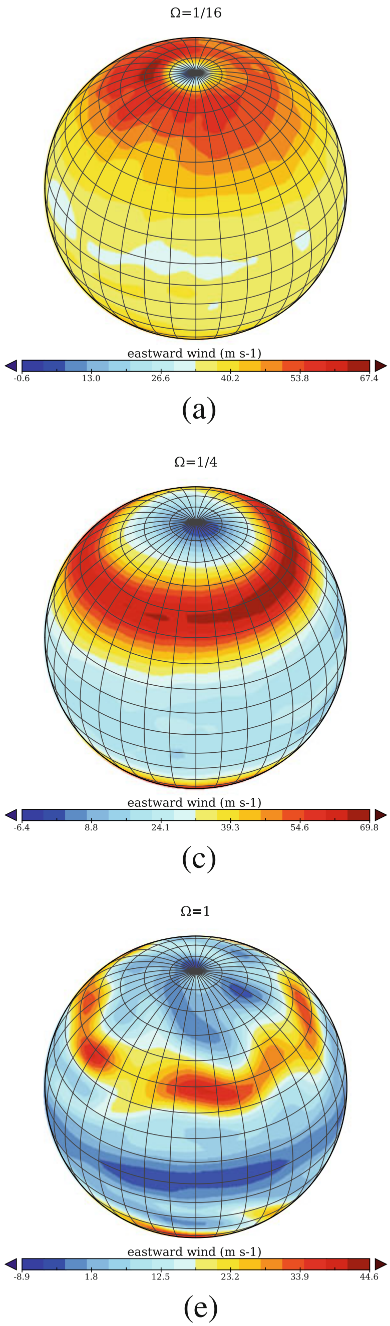

Fig. 9 Snapshots of upper level (200 hPa) zonal wind, projected onto a spherical surface at $\Omega^* = 1/16$ [(**a**)], 1/8 [(**b**)], 1/4 [(**c**)], 1/2 [(**d**)], 1 [(**e**)], and 2 [(**f**)], illustrating the basic organization of winds across the planet

zonal wavenumber to $m \sim 5-7$, much as observed on Earth. A further bifurcation evidently occurs between $\Omega^* = 1$ and 2, generating a second parallel meandering jet at a latitude around 60°, resulting in a complex zonally banded circulation.

Dimensionless Parameters

Although we can clearly order the sequence of atmospheric circulation regimes encountered in simplified model simulations according to physical parameters such as Ω^*, it is hard to make comparisons between these simulations and those, e.g., from models of planets of differing sizes, densities, or distances from their parent star. It may be more useful, therefore, to identify appropriate dimensionless parameters that play a major role in determining the form and intensity of atmospheric circulation regimes. These entail forming dimensionless combinations of physical parameters, such as those related to the size of the planet and its atmosphere, its rotation rate, and other physical attributes affecting processes such as buoyancy, radiative forcing, and friction.

The planetary radius, a, is the obvious length scale to take for the horizontal scale. Also, it is conventional to take as the vertical length scale the pressure scale height, $H = RT_0/g$, where R is the specific gas constant and T_0 a characteristic temperature. This might be justified theoretically on the grounds (Held 1978) that the scale height represents the maximum vertical scale over which baroclinic instability transports heat in a compressible atmosphere. A further aspect is that the horizontal and vertical temperature contrasts are not typically imposed directly by the applied solar heating or boundary conditions, but rather the typical scales for these quantities, $\Delta\theta_h$ and $\Delta\theta_v$ (where θ is potential temperature), are internal parameters, determined by the heat transports within the circulation itself. While it would be desirable in principle to be able to predict these quantities from the imposed insolation and planetary parameters, this problem is still incompletely understood (e.g., see Stone 1978; Schneider 2006; Zurita-Gotor and Lindzen 2007). So for the present we take the appropriate temperature scales as given from model simulations. Since the scale for the horizontal thermal contrast is taken along a near-isobaric surface or at the ground, it can be measured either in terms of absolute or potential temperature to within a factor of order unity (given $D \sim H$). With these modifications, we can define the following parameters, similar to those in Mitchell and Vallis (2010) and approximately equivalent to those found for laboratory systems (Geisler et al. 1983; Read et al. 2015),

$$\mathcal{R}o_T = \frac{R\Delta\theta_h}{\Omega^2 a^2} \quad \text{Thermal Rossby number} \tag{1}$$

$$\mathcal{B}u = \frac{R\Delta\theta_v}{2\Omega^2 a^2} \quad \text{Burger number} \tag{2}$$

based on a thermal wind scale

$$U_T = \frac{R\Delta\theta_h}{\Omega a}. \tag{3}$$

The thermal Rossby number is a convenient nondimensional measure of rotation, with low rotation rates corresponding to high thermal Rossby numbers. For example, in a sequence of experiments with an Earth-like model planet, Potter et al. (2014) found a strong dependence of super-rotation on $\mathcal{R}o_T$, with super-rotation consistently arising at thermal Rossby numbers of one and higher. The Burger number is a measure of the deformation radius, which we discuss more below.

Another characteristic horizontal length scale is the so-called Rhines scale, L_R, which represents the scale over which advection of relative and planetary vorticity is in balance (Rhines 1975; Vallis and Maltrud 1993). On the beta-plane, the Rhines scale is commonly expressed in terms of a wavenumber $k_R = 2\pi/\lambda_R \sim \sqrt{\beta/2U}$, where U is a turbulent velocity scale. If we use the above thermal wind scale to give U (thus making the strong, and potentially doubtful, assumption that the mean and eddy velocities are of the same order of magnitude) and take $\beta \sim \Omega/a$, then we obtain $k_R \simeq (2R\Delta\theta_h/\Omega^2)^{-1/2}$. This implies a length scale L_R corresponding to $\lambda_R/2$, equivalent to

$$L_R \simeq \frac{\pi}{k_R} = \pi \left(\frac{2R\Delta\theta_h}{\Omega^2}\right)^{1/2} \tag{4}$$

which we take here to be an estimate of the Rhines length scale. This scale is often found to be a reasonable estimate of the width or spacing, L_{jet}, of eddy-driven jets on a spherical planet or β-plane (e.g., Danilov and Gurarie 2002). The square of the ratio of the planetary radius to the Rhines scale is then given by

$$\mathcal{R}_h = \frac{a^2}{L_R^2} \simeq \frac{\Omega^2 a^2}{2R\Delta\theta_h} = \frac{1}{2\pi^2}\mathcal{R}o_T^{-1}, \tag{5}$$

i.e., $\mathcal{R}_h$ is proportional to the inverse of the thermal Rossby number. The smaller the thermal Rossby number, the more the number of zonal jets and/or baroclinic zones that might be expected, with the number of jets in each hemisphere scaling roughly as

$$N_J \simeq \frac{\pi a}{2L_R} \simeq \frac{\pi\sqrt{\mathcal{R}_h}}{2} = \frac{\mathcal{R}o_T^{-1/2}}{2\sqrt{2}}. \tag{6}$$

The significance of $\mathcal{R}o_T$ is further reinforced by the observation that the lateral scale, Y_H, predicted for the width of the Hadley circulation in the conceptual zonally symmetric model of Held and Hou (1980), is given by

$$Y_H = \left(\frac{5R\Delta\theta_h}{3\Omega^2}\right)^{1/2} = a\sqrt{\frac{5}{3}\mathcal{R}o_T}, \tag{7}$$

which assumes an angular momentum-conserving pattern of zonal wind in geostrophic balance. For slow rotation in which $\mathcal{R}o_T \gg 1$, the width of the Hadley circulation approaches the entire hemisphere of the planet itself, and one finds (Hou 1984)

$$Y_H \rightarrow \frac{\pi a}{2}\left(1 - \frac{3}{8\mathcal{R}o_T}\right), \tag{8}$$

again exhibiting a significant dependence on $\mathcal{R}o_T$.

The other major length scale that can be identified, and which is nominally independent of L_R, is the Rossby deformation radius, L_D. This is determined by the stratification $\Delta\theta_v$ rather than $\Delta\theta_h$. $\mathcal{B}u$ again measures the (squared) ratio of a representative average scale for L_D (taken here for $\phi \sim 45°$) to the planetary radius and may be expected to provide an indication of the likely importance of baroclinic instability in the circulation (applicable when $\mathcal{B}u$ is significantly less than 1).

Other parameters to be considered concern, e.g., the respective roles of friction and radiative damping, for which characteristic timescales, τ_f and τ_R, can be identified. Appropriate dimensionless measures of these quantities, analogous to the Taylor number, $\mathcal{T}_a$, in the laboratory (e.g., Read et al. 2015) and measuring the ratio of these timescales to that of planetary rotation, can be defined as

$$\mathcal{F}_r = 4(\Omega\tau_r)^4 \quad \text{Radiative damping} \tag{9}$$

$$\mathcal{F}_f = 4(\Omega\tau_f)^4 \quad \text{Frictional damping} \tag{10}$$

where the dominant of these parameters is likely to be the one with the lowest value. The planetary obliquity angle is another important parameter that determines the respective roles of seasonal changes and the geographical distribution of radiative forcing.

Circulation Regimes in Parameter Space

The trends in circulation regime presented in section "Circulation Regimes with Varying Rotation Rate" can now also be interpreted in the context of the dimensionless parameters introduced above. From the zonal mean temperature fields in Fig. 8, we can estimate typical values for $\Delta\theta_h$ and $\Delta\theta_v$, allowing a crude determination of $\mathcal{R}o_T$ and $\mathcal{B}u$. This also enables an estimate for N_J for comparison with the zonal wind fields in Fig. 8. Finally, given an estimate of the radiative time constant in the troposphere of around 10 Earth days and a surface drag timescale of around 2.5 days, we can also provide a rough indication of the smaller of the main dissipation parameters, $\mathcal{F}_f$. These estimates are listed for each of the cases shown in Figs. 8 and 9 in Table 3.

The onset of baroclinic instability for $\Omega^* > 1/4$ is consistent with an effective suppression of the instability beyond $\mathcal{R}o_T \sim 1.0$ and $\mathcal{B}u > 0.6$, which is broadly

Table 3 Key dimensionless parameters for the baseline set of numerical simulations with $\Delta\theta_h = 60$ K, $\tau_{ft} = 5$ Earth days, and $\tau_R = 25.9$ Earth days, as defined by Eqs. (1), (2), (10), (9), and (6), respectively

Ω^*	$\mathcal{B}u$	$\mathcal{R}o_T$	$\mathcal{F}_f$	$\mathcal{F}_r$	N_J
1/16	17.1	20.5	238	1.71×10^5	0.078
1/8	4.28	5.14	3.80×10^3	2.73×10^6	0.16
1/4	1.18	1.28	6.09×10^4	4.67×10^7	0.31
1/2	0.29	0.32	9.74×10^5	6.98×10^8	0.62
1	0.066	0.080	1.56×10^7	1.12×10^{10}	1.25
2	0.017	0.020	2.49×10^8	1.79×10^{11}	2.50

consistent with what is found in laboratory experiments (cf. Hide and Mason 1975; Read et al. 2015). However, one should be wary of overinterpreting such quantitative comparisons with systems that differ significantly from a planetary atmosphere in geometrical configuration, aspect ratio, and a variety of other parameters. In laboratory systems, for example, almost pure axisymmetric flow is found for $\mathcal{R}o_T > 1$, whereas in atmospheric simulations (e.g., Geisler et al. 1983; Del Genio and Suozzo 1987; Williams 1988a; Kaspi and Showman 2015; Wang et al. 2018), baroclinic instability may give way to forms of barotropic instability at low rotation rates, which seem to be much less efficient at transporting heat than their baroclinic counterparts. But this does at least indicate some broad, semiquantitative parallels that can be drawn with the laboratory analogues.

Such parallels extend further into the high rotation regimes, with a clear tendency for the formation of multiple zonal banded structures when $L_R \ll a$ and $\mathcal{R}_h \gg 1$. The corresponding estimate of numbers of zonal jets, given by N_J in Table 3, also seems to provide a fair guide as to the number of eastward and westward baroclinic jets appearing in each hemisphere, especially for $\Omega^* \gtrsim 1$. For the Earth-like case $\Omega^* = 1$, $N_J \sim 1-2$, suggesting that Earth is in an intermediate regime just beyond the situation where only a single jet in each hemisphere is favored.

Finally, we note that the frictional and radiative parameter estimates are all $\gg 1$, though not by such a large margin at low values of Ω^*. This may mean that the low rotation regimes represented in this sequence of simulations are relatively strongly damped, which should be borne in mind when comparing model results with real planetary atmospheres.

Discussion

We see from a range of model studies (Williams and Holloway 1982; Geisler et al. 1983; Del Genio and Suozzo 1987; Williams 1988a,b; Navarra and Boccaletti 2002; Mitchell and Vallis 2010; Kaspi and Showman 2015) that a parameter space can at least be constructed for hypothetical, somewhat idealized, circulations in Earth-like atmospheric systems, within which the style of circulation changes with Ω in ways that parallel those found in laboratory analogues quite closely. It is of interest,

Table 4 Estimates of the main dimensionless parameters for Earth, Mars, Pluto, Triton, Venus, and Titan, including the dimensionless super-rotation parameter s_{max}

Body	$\mathcal{B}u$	$\mathcal{R}o_T$	N_J	s_{max}
Earth	0.02	0.06	1.26	$\lesssim$0.04
Mars	0.04	0.20	0.92	0.16
Pluto	163	4.8	0.16	0.75–1.1
Triton	22.4	1.05	0.35	0.3–0.6
Titan	11.8	18	0.06	8.5–15
Venus	140	370	0.009	55–65

therefore, to look further into where the terrestrial planets amenable to study in the solar system might lie within the parameter space we have constructed.

Table 4 presents some approximate estimates of the key dimensionless parameters discussed above for Earth, Mars, Pluto, Triton, Venus, and Titan, for comparison with the model simulations discussed in the previous section. From this, we see that these six terrestrial planetary bodies fall into three main groups. The first contains Mars and Earth, both with values of $\mathcal{R}o_T < 1$ and forming a group of relatively rapid rotators. Given the relatively small values of $\mathcal{R}o_T$, we would anticipate relatively narrow tropical Hadley circulations (Held and Hou 1980) and baroclinically active midlatitudes, much as observed. Moreover, the relative values of $\mathcal{R}o_T$ for Earth and Mars in Table 4 would suggest (a) that Mars's tropical Hadley circulation would likely extend to higher latitudes than on Earth, by a factor $\sim\sqrt{3}$, and (b) baroclinic instability on Earth is likely to be more strongly supercritical and on a smaller scale relative to the planet than on Mars. From a comparison of Figs. 1 and 2, it is clear that (a) is borne out quite accurately, with Hadley cells extending to around 30–40° on Earth and up to 60° on Mars. For (b) also, baroclinic instability on Mars is known to favor relatively low planetary wavenumber features ($m = 1$–3 typically; Read and Lewis 2004) with baroclinic storms disappearing altogether during part of the seasonal cycle in each hemisphere, whereas on Earth, wavenumbers around $m = 4$–8 are more typical and persist throughout the year.

The second group contains Venus and Titan as extreme members, for which $\mathcal{R}o_T \gg 1$, consistent with slowly rotating atmospheres in predominantly cyclostrophic or gradient wind balance that are likely to support barotropic instabilities in preference to baroclinic eddy processes. This group also seems consistently to exhibit strong values of super-rotation s, broadly consistent with the model simulations in section "Circulation Regimes with Varying Rotation Rate" though the quantitative agreement between models and observations may be less close than this comparison would suggest. The Hadley circulations in the slowly rotating model simulations in the previous section were also found to extend almost to the poles which, again, seem consistent with the Venus-like simulation illustrated in Fig. 3 and other evidence, e.g., from Venus observations and model simulations of Titan (Sánchez-Lavega et al. 2017; Lebonnois et al. 2012).

The third group contains Pluto and Triton, for which $\mathcal{R}o_T \sim 1$, indicative also of non-geostrophic flow and broad Hadley cells in an extended tropical zone. The available GCM simulations to date suggest relatively weak winds in both atmospheres. This may reflect the strongly dissipative states of both atmospheres, for which molecular viscosity may play a much stronger role than on other terrestrial planets in the solar system because of the very low surface pressure, comparable to thermospheric pressures on Earth and other terrestrial planets. Another factor peculiar to both of these atmospheres is their tendency to condense and evaporate the main atmospheric constituent (N_2) on seasonal timescales, leading to a strong circulation transferring mass from the evaporating summer polar ice cap toward the condensing cap over the winter pole associated with zonal flows through deflection of such pole-pole circulations by Coriolis forces. Such effects are likely to be fairly extreme for Pluto, whose obliquity is nearly 120° and whose orbital period is extremely long (∼248 Earth years), allowing time for a large fraction of Pluto's tenuous atmosphere to condense out during winter.

The radiative damping parameter, $\mathcal{F}_r$, is another factor where some of the solar system planets lie some significant distance away from the model simulations in our parameter space. Mars in particular is likely to be significantly more strongly dissipative than both the corresponding model cases ($\Omega^* = 1/2-1/4$; with roughly 2–3 times the values of $\mathcal{R}o_T$ and $\mathcal{B}u$ as for Earth itself). By analogy with the laboratory systems discussed above (Hide and Mason 1975; Read et al. 2015), this would suggest the likelihood that baroclinic instabilities on Mars would be more strongly dissipative and hence less strongly supercritical and nonlinear. Such a condition is consistent with a tendency to favor smaller planetary wavenumber structures that are relatively coherent and long-lived, with comparatively simple time variations. This is consistent with a lot of evidence on Mars from both models and observations that baroclinic activity on Mars is relatively coherent and periodic (Barnes 1980, 1981; Collins et al. 1996).

The location of planets in this basic parameter space thus seems to provide a number of useful insights that can account for a variety of different features found on the terrestrial planets within the solar system, including the size of the Hadley circulation and the nature of large-scale waves and instabilities that may develop within the circulation. It also indicates the validity and possible utility of the concept of dynamical similarity, widely used in fluid mechanics, which anticipates that circulating fluid systems of differing sizes, with different rotation rates, thermal properties, etc., will organize themselves in similar ways if a set of key dimensionless parameters are of similar magnitudes. In the present problem, this would seem to imply similarity provided $\mathcal{R}o_T$ is matched between two different planetary circulations, together with some other parameters, e.g., related to the dissipation and radiative timescales. This was clearly illustrated in a recent study by Pinto and Mitchell (2014) for a slowly rotating planetary circulation, in which they compared simple model simulations obtained either for an Earth-sized planet rotating with a period of 20 Earth days or for a planet 1/20 the radius of Earth rotating with a period of 1 day. The results are illustrated in Fig. 10, in which (a) and (b) are shown for $\Omega^* = 1/20$ and (c) and (d) are shown for $a = a_{Earth}/20$, $\mathcal{R}o_T = 1.3$ for both cases, however, and the resulting fields of zonal mean velocity and temperature are very similar in both structure and amplitude. Some caution is necessary in making this comparison, however, since this degree of similarity

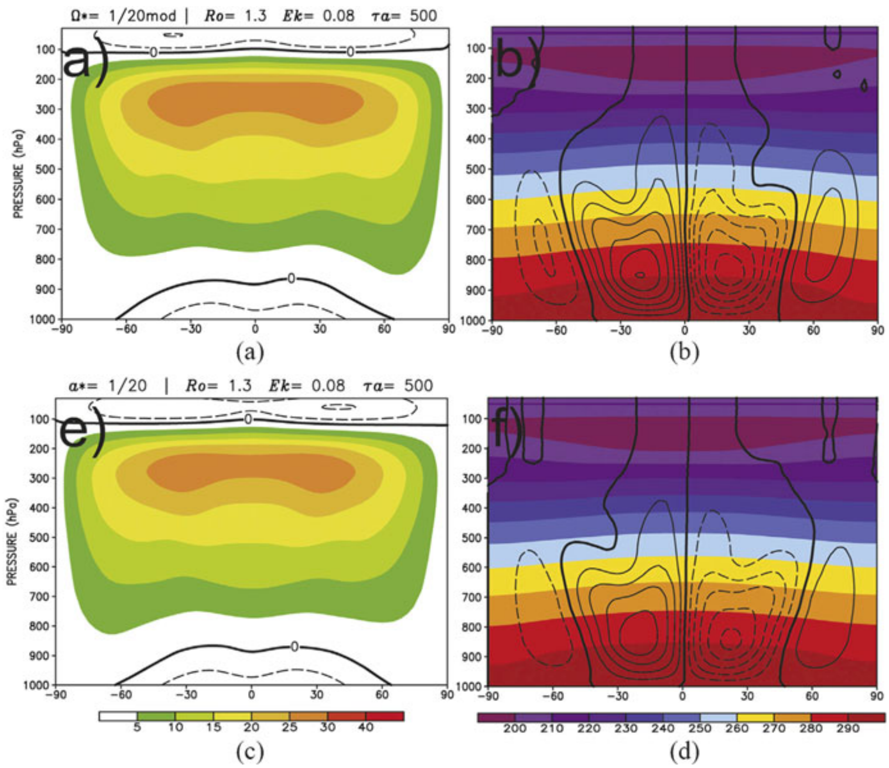

Fig. 10 An illustration of the potential for dynamical similarity between the atmospheric circulations of two planets with differing radii and rotation rates but with common values of $\mathcal{R}o_T = 1.3$ and dissipation parameters. Panels a and b are for an Earth-sized planet rotating at 1/20 of the Earth's rotation rate, while panels c and d are for a planet 1/20th the size of Earth rotating at the same speed as Earth. Panels a and c show the zonal wind velocity (in m s^{-1}) and panels b and d show the corresponding zonal mean temperature field (color shaded) and meridional mass stream function (line contours). (Figures taken from Pinto and Mitchell 2014 with permission from Elsevier)

also required the models to match dissipation and radiative damping parameters, $\mathcal{F}_f$ and $\mathcal{F}_r$ (represented in Pinto and Mitchell 2014 by $Ek = (4\mathcal{F}_f)^{-1/4}$ and $\tau_a = (4\mathcal{F}_r)^{1/4}$) as well as $\mathcal{R}o_T$. Similarity of obliquity would also be necessary in practice, and several other parameters, e.g., involving the thermodynamic properties of the atmosphere and its composition, though similarity of these four main parameters would be likely to capture most of the gross properties of the circulation.

Prediction From Dynamical Similarity

This potential for dynamical similarity therefore suggests the possibility of predicting certain aspects of planets that are yet to be discovered, provided their position in dimensionless parameter space can be established. As an example, consider a hypothetical "super-Earth" with a mass around 8–10 $M_{\oplus}$, rotating about its axis at about the same angular velocity as Earth itself and in orbit around a star within its "habitable zone." Provided the obliquity of such a planet were not too large, we would anticipate the circulation to be largely determined by the value of $\mathcal{R}o_T$, which scales as $(\Omega a)^{-2}$, where a would be around twice Earth's radius. For a value of Ω comparable to what occurs on Earth, therefore, this would indicate a circulation pattern roughly equivalent to the $\Omega^* = 2$ case presented in the previous section. This would suggest a more complicated circulation than on Earth with at least two distinct, parallel baroclinic storm zones at midlatitudes and a relatively narrow tropical Hadley circulation extending only to around 15° in latitude from the equator. Westward winds would be expected to dominate near the equator and around 60°, with eastward zonal winds elsewhere. If moisture is also taken into account in this circulation, as potentially appropriate for a "waterworld" super-Earth (Selsis et al. 2007), these models could even be used to predict climatological regions of high and low rainfall (e.g., with low rainfall at the poleward edge of the Hadley cell).

Tidally Locked Planets

Although such ideas of dynamical similarity should apply generically to wide classes of non-synchronously rotating planets, many recently discovered exoplanets are located in orbits very close to their parent stars. The strong gravitational tidal interactions between star and planet would then be likely to force the rotation of the planet into a synchronous state, in which the rotation and orbital periods are in the ratio of simple integers, such as for Mercury in our solar system, for which the ratio is 3:2 (Pettengill and Dyce 1965; McGovern et al. 1965), with a relatively small obliquity. For closer-in planets, a 1:1 ratio is more likely with an obliquity close to zero, analogous to the Earth-Moon system, so that the planet permanently presents the same face to the star.

Under these conditions, the atmospheric circulation would be rather different in form to the non-synchronously rotating cases discussed above (e.g., see Joshi et al. 1997; Joshi 2003), with a dominant circulation transporting air in longitude from the substellar point to the anti-stellar point, as well as from the equator to poles. Recent studies (e.g., Showman et al. 2010; Penn and Vallis 2017) have shown that the circulation under these circumstances may be dominated by a stationary pattern of dynamically coupled planetary waves (mainly equatorial Kelvin and Rossby waves, possibly resembling the Gill pattern; Gill (1980); Vallis (2017) in association with a strongly prograde equatorial zonal jet stream. However, tidal locking may be prevented by thermal tides in sufficiently massive atmospheres (Ingersoll and Dobrovolskis 1978; Leconte et al. 2015), and relative strengths of the stationary wave pattern and zonal jet also depend upon factors such as the actual rotation rate, the stratification (and hence the radius of deformation), and the overall mass of the atmosphere. As with solar system planets, idealized simulations can give insight and two examples are shown in Fig. 11. These show simulations with a primitive equation model in a tidally locked state (left panel) and a state in which the substellar

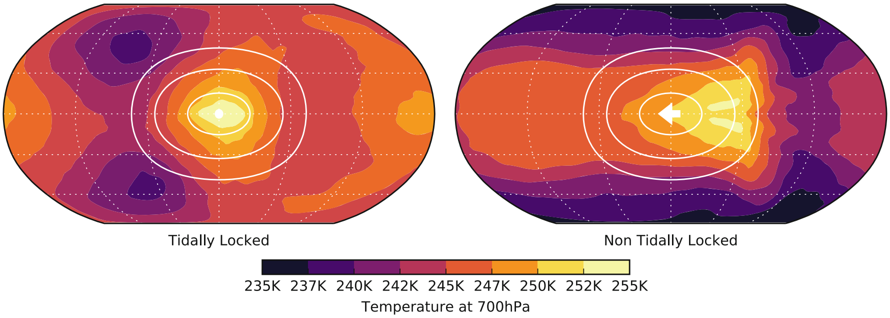

Fig. 11 Primitive equation simulations of tidally locked (left) and nontidally locked (right) exoplanets, with forcing via thermal relaxation to a specified field. Color shading shows the temperature at 700 hPa and white contours show the location of the thermal forcing. For the nontidally locked case, the substellar point is shown with a small white arrow denoting its direction of passage, which is to the left, here with a velocity of 25 m s^{-1}. (Figure from Vallis et al. 2018)

point traverses the planet from right to left (right panel). In the tidally locked state, Rossby lobes can be seen to the west and poleward of the heating, as in the Gill pattern. Interestingly, the hotspot in the nontidally locked case is not synchronous with the maximum of the thermal forcing (the substellar point), and the investigation of this continues.

Understanding and quantifying the balance between stationary wave patterns and zonal flows is important for interpreting observations of close-in extrasolar planets, since it affects the thermal contrast between the substellar and anti-stellar hemispheres which can be deduced from observed phase curves (e.g., Crossfield 2015). A number of studies have begun to explore the sensitivity of the synchronously locked circulation of close-in planetary atmospheres to various parameters (e.g., Merlis and Schneider 2010; Edson et al. 2011; Carone et al. 2015, 2016; Showman et al. 2015; Penn and Vallis 2017; Noda et al. 2017), although a complete picture of the relevant parameter space is yet to emerge. But progress so far indicates that such an approach using idealized numerical simulations, combining basic dynamical theory with the identification of the key dimensionless parameters, is well worthwhile.

Acknowledgements Thanks are due to the many colleagues and students who have contributed to our understanding of this subject and carried out some of the research described herein, particularly Raymond Hide, Sebastien Lebonnois, James Penn, Fachreddin Tabataba-Vakili, Yixiong Wang, and Gareth Williams. GKV also acknowledges support from the Leverhulme Trust.

References

Andrews DG, Holton JR, Leovy CB (1987) Middle atmosphere dynamics. Academic, New York

Barnes JR (1980) Time spectral analysis of mid-latitude disturbances in the Martian atmosphere. J Atmos Sci 37:2002–2015

Barnes JR (1981) Midlatitude disturbances in the Martian atmosphere: a second Mars year. J Atmos Sci 38:225–234

Bastin M, Read PL (1998) Experiments on the structure of baroclinic waves and zonal jets in an internally heated rotating cylinder of fluid. Phys Fluids 10:374–389

Beaulieu JP et al (2006) Discovery of a cool planet of 5.5 Earth masses through gravitational microlensing. Nature 439:437–440

Bourke W (1974) A multilevel spectral model. I. Formulation and hemispheric integrations. Mon Weather Rev 102:687–701

Carone L, Keppens R, Decin L (2015) Connecting the dots – II: phase changes in the climate dynamics of tidally locked exoplanets. Mon Not R Astr Soc 453:2412–2437

Carone L, Keppens R, Decin L (2016) Connecting the dots – III: nightside cooling and surface friction affect climates of tidally-locked terrestrial planets. Mon Not R astr Soc 461:1981–2002

Collins M, Lewis SR, Read PL, Hourdin F (1996) Baroclinic wave transitions in the martian atmosphere. Icarus 120:344–357

Crossfield IJM (2015) Observations of exoplanet atmospheres. Pub Astron Soc Pac 127:941–960

Danilov S, Gurarie D (2002) Rhines scale and the spectra of β-plane turbulence with bottom drag. Phys Rev E 65:067301

Dee DP, Uppala SM, Simmons AJ et al (2011) The ERA-interim reanalysis: configuration and performance of the data assimilation system. Quarterly Q J R Meteorol Soc 137(656):553–597

Del Genio A, Suozzo RJ (1987) A comparative study of rapidly and slowly rotating circulation regimes in a terrestrial general circulation model. J Atmos Sci 44:973–986

Edson A, Lee S, Bannon P, Kasting JF, Pollard D (2011) Atmospheric circulation of terrestrial planets orbiting low mass stars. Icarus 212:1–13

Forget F, Bertrand T, Vangvichith M, Leconte J, EM Lellouch E (2017) A post-New Horizons global climate model of Pluto including the N_2, CH_4 and CO cycles. Icarus 287:54–71

Fraedrich K, Kirk E, Lunkeit F (1998) Puma: Portable University Model of the Atmosphere. Deutsches Klimarechenzentrum Technical Report 16

Frisius T, Lunkeit F, Fraedrich K, James IN (1998) Storm-track organization and variability in a simplified global circulation model. Quart J R Meteor Soc 124:1019–1043

Fultz D, Long RR, Owens GV et al. (1959) Studies of thermal convection in a rotating cylinder with some implications for large-scale atmospheric motions. Meteorological monographs, vol 4. American Meteorological Society, Boston

Geisler JE, Pitcher EJ, Malone RC (1983) Rotating-fluid experiments with an atmospheric general circulation model. J Geophys Res 88:9706–9716

Ghil M, Childress S (1987) Topics in geophysical fluid dynamics: atmospheric dynamics, dynamo theory and climate dynamics. Springer, New York

Gill AE (1980) Some simple solutions for heat induced tropical circulation. Quart J R Meteorol Soc 106:447–462

Held IM (1978) The vertical scale of an unstable baroclinic wave and its importance for eddy heat flux parameterizations. J Atmos Sci 35:572–576

Held IM, Hou AY (1980) Nonlinear axially symmetric circulations in a nearly inviscid atmosphere. J Atmos Sci 37:515–533

Hide R (1953) Some experiments on thermal convection in a rotating liquid. Quart J R Meteorol Soc 79:161

Hide R, Mason PJ (1975) Sloping convection in a rotating fluid. Adv Phys 24:47–99

Hoskins BJ, Simmons AJ (1975) A multi-layer spectral model and the semi-implicit method. Quart J R Meteor Soc 101:637–655

Hou AY (1984) Axisymmetric circulations forced by heat and momentum sources: a simple model applicable to the Venus atmosphere. J Atmos Sci 41:3437–3455

Hubbard WB, Yelle RV, Lunine JL (1990) Nonisothermal Pluto atmosphere models. Icarus 84:1–11

Ingersoll AP, Dobrovolskis AR (1978) Venus' rotation and atmospheric tides. Nature

Jenkins GS (1996) A sensitivity study of changes in Earth's rotation rate with an atmospheric general circulation model. Glob Plan Change 11:141–154

Joshi MM (2003) Climate model studies of synchronously rotating planets. Astrobiology 3:415–427
Joshi MM, Haberle RM, Reynolds RT (1997) Simulations of the atmospheres of synchronously rotating terrestrial planets orbiting M Dwarfs: conditions for atmospheric collapse and the implications for habitability. Icarus 129:450–465
Kållberg P, Berrisford P, Hoskins B et al. (2004) ERA-40 atlas. ERA40 Project Reports Series 19, ECMWF
Kaspi Y, Showman AP (2015) Atmospheric dynamics of terrestrial exoplanets over a wide range of orbital and atmospheric parameters. Astrophys J 804:60
Kraucunas I, Hartmann DL (2005) Equatorial superrotation and the factors controlling the zonal-mean zonal winds in the tropical upper troposphere. J Atmos Sci 62:371–389
Lebonnois S, Hourdin F, Eymet V et al (2010) Superrotation of Venus' atmosphere analyzed with a full general circulation model. J Geophys Res 115:E06006
Lebonnois S, Burgalat J, Rannou P, Charnay B (2012) Titan global climate model: a new 3-dimensional version of the IPSL Titan GCM. Icarus 218(1):707–722
Lebonnois S, Sugimoto N, Gilli G (2016) Wave analysis in the Venus atmosphere below 100-km, simulated by the LMD Venus GCM. Icarus 278:38–51
Leconte J, Wu H, Menou K, Murray N (2015) Asynchronous rotation of Earth-mass planets in the habitable zone of lower-mass stars. Science 347:632–635
Leovy CB (1973) Rotation of the upper atmosphere of Venus. J Atmos Sci 30:1218–1220
Lewis S, Read P (2003) Equatorial jets in the dusty Martian atmosphere. J Geophys Res E: Planets 108(4):15
Lewis SR, Collins M, Read PL et al (1999) A climate database for Mars. J Geophys Res 104:24177–24194
Lorenz EN (1969) The nature and theory of the general circulation of the atmosphere. T. P. 115, No. 218, W. M. O., Geneva
Lorenz EN (1993) The essence of chaos. UCL Press, London
Mayor M, Udry S, Lovis C et al (2009) The HARPS search for southern extra-solar planets XIII. A planetary system with 3 super-Earths (4.2, 6.9, and 9.2 $M_{\oplus}$). Astron Astrophys 493:639–644
McGovern WE, Gross SH, Rasool SI (1965) Rotation period of the planet Mercury. Nature 208:375
Merlis TM, Schneider T (2010) Atmospheric dynamics of Earth-like tidally locked aquaplanets. J Adv Model Earth Syst 2:13
Mitchell J, Vallis GK (2010) The transition to superrotation in terrestrial atmospheres. J Geophys Res (Planets) 115:E12,008, 17
Navarra A, Boccaletti C (2002) Numerical general circulation experiments of sensitivity to Earth rotation rate. Climate Dyn 19:467–483
Noda S, Ishiwatari M, Nakajima K et al (2017) The circulation and day-night heat transport in the atmosphere of a synchronously rotating aquaplanet: dependence on planetary rotation rate. Icarus 282:1–18
Penn J, Vallis GK (2017) The thermal phase curve offset on tidally and nontidally locked exoplanets: A shallow water model. Astrophys J 842(2):101. http://stacks.iop.org/0004-637X/842/i=2/a=101
Pettengill GH, Dyce RB (1965) A radar determination of the rotation of the planet Mercury. Nature 206:1240
Pinto JRD, Mitchell JL (2014) Atmospheric superrotation in an idealized GCM: parameter dependence of the eddy response. Icarus 238:93–109
Potter SF, Vallis GK, Mitchell JL (2014) Spontaneous superrotation and the role of Kelvin waves in an idealized dry GCM. J Atmos Sci 71(2):596–614
Read PL (1986) Super-rotation and diffusion of axial angular momentum: II. A review of quasi-axisymmetric models of planetary atmospheres. Quart J R Meteorol Soc 112:253–272
Read PL (2001) Transition to geostrophic turbulence in the laboratory, and as a paradigm in atmospheres and oceans. Surv Geophys 22:265–317
Read PL, Lebonnois S (2018, in press) Super-rotation on Venus, Titan and elsewhere. Ann Rev Earth Plan Sci 46

Read PL, Lewis SR (2004) The Martian climate revisited: atmosphere and environment of a desert planet. Springer-Praxis, Berlin/Heidelberg/New York

Read PL, Pérez EP, Moroz IM, Young RMB (2015) General circulation of planetary atmospheres: insights from rotating annulus and related experiments. In: von Larcher T, Williams PD (eds) Modelling atmospheric and oceanic flows: insights from laboratory experiments and numerical simulations. American Geophysical Union/Wiley, Hoboken, pp 9–44

Rhines PB (1975) Waves and turbulence on a β-plane. J Fluid Mech 69:417–443

Sánchez-Lavega A, Lebonnois S, Imamura T, Read P, Luz D (2017) The atmospheric dynamics of Venus. Space Sci Rev 212:1541–1616

Saravanan R (1993) Equatorial superrotation and maintenance of the general circulation in two-level models. J Atmos Sci 50:1221–1227

Schneider T (2006) The general circulation of the atmosphere. Ann Rev Earth Plan Sci 34:655–688

Selsis F, Kasting JF, Levrard B et al (2007) Habitable planets around the star Gliese 581? Astron Astrophys 476:1373–1387

Showman AP, Cho J, Menou K (2010) Atmospheric circulation of extrasolar planets. In: Seager S (ed) Exoplanets. University of Arizona Press, Arizona, pp 471–516

Showman AP, Lewis NK, Fortney JJ (2015) Three-dimensional atmospheric circulation of warm and hot Jupiters: effects of orbital distance, rotation period and nonsynchronous rotation. Astrophys J 801:95

Stone P (1978) Baroclinic adjustment. J Atmos Sci 35:561–571

Suarez MJ, Duffy DG (1992) Terrestrial superrotation: a bifurcation of the general circulation. J Atmos Sci 49:1541–1554

Udry S, Bonfils X, Delfosse X et al (2007) The HARPS search for southern extra-solar planets XI. Super-Earths (5 and 8 $M_{\oplus}$) in a 3-planet system. Astron Astrophys 469:L43–L47

Vallis GK (2016) Geophysical fluid dynamics: whence, whither and why? Proc Roy Soc A 472: 1–23

Vallis GK (2017) Atmospheric and oceanic fluid dynamics: fundamentals and large-scale circulation, 2nd edn. Cambridge University Press, Cambridge

Vallis GK, Maltrud ME (1993) Generation of mean flows and jets on a beta plane and over topography. J Phys Oceanog 23:1346–1362

Vallis GK, Colyer G, Geen R et al (2018) Isca, v1.0: a framework for the global modeling of the atmospheres of Earth and other planets at varying levels of complexity. Geosci Model Dev 11:843–859 https://doi.org/10.5194/gmd-11-843-2018

von Hardenberg J, Fraedrich K, Lunkeit F, Provenzale A (2000) Transient chaotic mixing during a baroclinic life cycle. Chaos 10:122–134

Wang Y, Read PL, Tabataba-Vakili F, Young RMB (2018) Comparative terrestrial atmospheric circulation regimes in simplified global circulation models: I. From cyclostrophic super-rotation to geostrophic turbulence. Quart J R Meteorol Soc submitted

Williams GP (1988a) The dynamical range of global circulations – I. Clim Dyn 2:205–260

Williams GP (1988b) The dynamical range of global circulations – II. Clim Dyn 3:45–84

Williams GP (2003) Barotropic instability and equatorial superrotation. J Atmos Sci 62:2136–2152

Williams GP, Holloway JL (1982) The range and unity of planetary circulations. Nature 297: 295–299

Wordsworth RD, Read PL, Yamazaki YH (2008) Turbulence, waves and jets in a differentially heated rotating annulus experiment. Phys Fluids 20:126602. https://doi.org/10.1063/1.2990,042

Yelle RV, Lunine JL, Pollack JB, Brown RH (1995) Lower atmospheric structure and surface-atmosphere interactions on Triton. In: Cruikshank DP, Matthews MS Schumann AM (eds) Neptune and triton. University of Arizona Press, Tucson, pp 1031–1105

Zalucha AM (2016) An atmospheric general circulation model for Pluto with predictions for New Horizons temperature profiles. Mon Not R astr Soc 459:902–923

Zalucha AM, Michaels TI (2013) A 3D general circulation model for Pluto and Triton with fixed volatile abundance and simplified surface forcing. Icarus 223:819–831

Zurita-Gotor P, Lindzen R (2007) Theories of baroclinic adjustment and eddy equilibration. In: Schneider T, Sobel A (eds) The global circulation of the atmosphere: phenomena, theory, challenges. Princeton University Press, Princeton